Hindawi
Journal of Chemistry
Volume 2020, Article ID 6724157, 12 pages
https://doi.org/10.1155/2020/6724157

Research Article

Effect Factor of Arsenite and Arsenate Removal by a Manufactured Material: Activated Carbon-Supported Nano-TiO_2

Qian Luo,[1,2] Gang Li,[1,2] Meifeng Chen,[1,2] Fanxin Qin,[1,3] Haiyan Li,[1,2] and Yu Qiang[1,2]

[1]*College of Life Sciences, Guizhou Normal University, Huaxi District, Guiyang 550025, Guizhou Province, China*
[2]*Provincial Key Laboratory for Information System of Mountainous Areas and Protection of Ecological Environment, Guizhou Normal University, Yunyan District, Guiyang 550001, Guizhou Province, China*
[3]*Key Laboratory of State Forestry Administration on Biodiversity Conservation in Karst Mountainous Areas of Southwestern China, Guizhou Normal University, Huaxi District, Guiyang 550025, Guizhou Province, China*

Correspondence should be addressed to Fanxin Qin; qinfanxin@gznu.edu.cn

Received 28 April 2020; Revised 1 July 2020; Accepted 29 July 2020; Published 18 September 2020

Academic Editor: Gulaim A. Seisenbaeva

Copyright © 2020 Qian Luo et al. This is an open access article distributed under the Creative Commons Attribution License, which permits unrestricted use, distribution, and reproduction in any medium, provided the original work is properly cited.

Carbon substrate-supported nano-TiO_2 (a manufactured material) was prepared in this study for arsenic removal. The removal rates of arsenic were evaluated by batch tests under several simulation conditions including pH, ionic strength, and adsorbent dosage. Results showed that As(III) and As(V) adsorption reached equilibrium within 10 hours (pH = 8 and ionic strength 0.5 mol/L). At pH = 8, maximum adsorption efficiency was discovered for the adsorbent. Removal rate was proportional to the increase in ionic strength. The removal data were satisfactorily fitted to the pseudo-second-order kinetic model ($R^2 > 0.9990$) and Freundlich equation ($R^2 \geq 0.9600$) for adsorption thermodynamic behaviors. New material showed more effective adsorption performance for As(V) than for As(III). It was found that 15.1800 mg/g As(V) and 13.3800 mg/g As(III) were adsorbed, respectively. In addition, material properties were studied including the structure of crystallinity, surface morphology, functional groups, and surface texture by XRD, TEM/SEM, FTIR, and BET methods, respectively. XRD result showed supported nano-TiO_2 had the anatase phase. The size of the microparticle was around 52 nm. BET results indicated that material surface areas, pore volume, and pore size diameter were 371.17 m^2/g, 0.35 cm^3/g, and 11.70 nm, respectively. FTIR spectrum indicated that several functional groups (OH^-, Ti-O) existing in supported nano-TiO_2 may facilitate the adsorption efficiency. Mechanistically, supported nano-TiO_2 played a key role in promoting adsorption efficiency and converting As(III) to As(V). Results indicated that the investigated adsorbents possessed an excellent arsenic removal capability.

1. Introduction

Arsenic (As) is a metalloid element, which exists in the form of arsenite As(III) and arsenate As(V) [1, 2] and can be widely detected in both natural and anthropogenic sources [3]. A close attention has been paid to its serious threats to humans and animals due to its high toxicity [4, 5]. In environmental pollution aspects, both As(III) and As(V) have been discovered in soil, organisms, and water and mobilized through a combination of natural processes such as weathering reactions, biological activity, and volcanic emissions [6]. For anthropogenic activities, arsenic contamination has been mainly caused by combustion of fossil fuels, petroleum refineries, mining, and nonferrous smelting activity [7–9]. In China, there are different degrees of arsenic exposure in the living environment of residents, and the arsenic pollution in drinking water has exceeded the threshold level (10 μg/L) [10]. Therefore, how to effectively remove arsenic or make a conversion from As(III) to As(V) by the highest oxidation rate for reducing its toxicity and detriments is a key issue in arsenic pollution control and treatment.

A large number of physical-chemical treatment processes were applied to remove toxicity elements in water and alleviate water pollution, including in precipitation, ion-exchange, adsorption, and membrane filtration [11–16]. Among them, adsorption is one of the most preeminent removal methods because of the low cost, ease of operation, and high efficiency [17]. Higher efficiency of

arsenic removal can be finished by adsorbing arsenic or converting As(III) to As(V) through the preoxidation process indirectly since As(III) was difficult to remove by most techniques directly.

Titanium dioxide [18] and its modified counterparts [19] showed excellent removal efficiencies by adsorbing arsenic from water. In brief, the mechanism of adsorption can be attributed to their special physical and chemical properties: high theoretical adsorption capacity, larger specific surface area, oxidation behavior, photocatalytic efficiency, and high affinity of surface hydroxyl groups [20]. In addition, particle sizes of the adsorbent affect adsorption capacity for arsenic [18]. Bang et al. [21] found that the arsenic species had a high affinity with the surface sites of TiO_2. Although TiO_2-doped materials have excellent adsorption performance, their limited load may hinder the extensive application of traditional prepared nano-TiO_2-doped materials. Long and Tu [22] conducted arsenic removal by activated carbon-supported granular nano-TiO_2, but they found nano-TiO_2 loaded amount was too low to decease the As level. To improve the loaded amount of nano-TiO_2, tetrabutyl titanate doped with activated carbon powder was produced by the sol-gel method in our experiment.

In the study, a new adsorbent was prepared and devoted to remove As(III) and As(V) in aqueous solution. The effects of pH, adsorbent dosage, and ionic strength are elucidated to explore the optimum removal conditions. Adsorption kinetics and isotherms were investigated to probe the adsorption efficiency and maximum adsorption capacity for arsenic. The main objectives of this research were (a) to produce an adsorption material with preloading TiO_2 sufficiently and good uniformity, (b) adsorb arsenic by the material and determine its maximum adsorption capacity of As(III) and As(V), and (c) explain the adsorption mechanism of the material.

2. Materials and Methods

2.1. Materials and Agents. Nitric acid (HNO_3), anhydrous ethanol (C_2H_5OH), tetrabutyl titanate ($C_{16}H_{36}O_4Ti$), and glacial acetic acid (CH_3COOH) were purchased from Sinopharm Chemical Reagent Co., Ltd (China). Ammonium sulfate ($(NH_4)_2SO_4$, analytical reagent) was supplied by Tianjin Kermel Chemical Reagent Co., Ltd (China). Activated carbon powder was obtained from Hunan Deban Activated Carbon Co., Ltd (China). $NaAsO_2$ was a source of 1000 mg/L As(III). 1000 mg/L As(V) was prepared by the oxidation of stock solution of As(III) using excess potassium peroxydisulfate ($K_2S_2O_8$). NaCl, NaOH (0.1 mol/L), and HCl (0.1 mol/L) solutions were prepared by using deionized water (18.2 MΩ·cm). Stock solutions were stored in dark before experiments. Unless otherwise stated, all chemicals are of analytical grade and above.

2.2. Adsorbent Preparation and Characterization

2.2.1. Adsorbent Preparation. The adsorbent preparation was based on Rong et al.'s study [23], and the detailed procedure is as follows:

(1) *Pretreatment of Activated Carbon*. Certain amount of activated carbon powder (16.4 g) was presoaked by HNO_3 and then added into the mixture of 70 mL anhydrous C_2H_5OH and 20 mL tetrabutyl titanate under pH 2-3 (adjusted by glacial acetic acid).

(2) *Preparation of Solution A*. Anhydrous C_2H_5OH (20 mL), 60 mL water, and 2.4 g ammonium sulfate were prepared in a cleaning breaker, and then acetic acid was used to regulate pH in the range of 2-3, getting B solution.

(3) *Preparation of Carbon Substrate-Supported Nano-TiO_2*. Solution A was dripped to pretreated activated carbon in speeded stirring process (200 r/min) and continued to stir for 2 hours at room temperature (25~28°C). These solutions were placed in an oven at 100°C for 24 hours, and after the dried material was grounded, it was placed in a muffle furnace and calcined at 500°C for 2 hours and then naturally cooled down to room temperature to form adsorption material eventually.

2.2.2. Material Characterization. New material was characterized by XRD, TEM/SEM, FTIR, and BET methods, respectively. The X-ray diffractometer (XRD, DY2862, Holland) was applied to explore the crystal structure of materials. Transmission electron microscope (TEM, JEM-2100F, Japan) and scanning electron microscope (SEM, JSM-6490LV, Japan) determined shapes of the adsorbent. The functional groups of the adsorbent were observed by the Fourier-transform infrared spectrometer (FTIR, TENSOR27, Bruker, Germany). 3H-2000IIIA surface analysis meter (Beishide Instrument Technology Co., Ltd., China) was used to measure BET (Brunauer–Emmett–Teller) specific surface area, pore diameter, and pore volume. Titanium content was determined by ICP-OES (Optima 5300V, PerkinElmer, USA), and TiO_2 loaded amount was calculated.

2.3. Batch Adsorption Experiments. All glassware and polyethylene bottles were acid-soaked by 10% HNO_3 at least 24 h before each experiment and then washed three times with distilled water and dried in the oven. NaCl was used to adjust the ionic strength of solution, HCl and NaOH (both 0.1 mol/L) were used for the required pH adjustment, and pH values were measured by using a pH meter (3E, Shanghai Leici Inc., China). The zeta potential was determined by a Zetasizer (Zetasizer Nano ZS, Malvern Instrument, UK). 1000 mg/L As(III) and As(V) solution was diluted into the required concentration solutions, then volume of the reaction was selected as 25 mL, and appropriate dosage of the adsorbents was added, adsorbed for a proper time at room temperature (25~28°C), and centrifuged 30 minutes (4000 r/min) after it settled 20 minutes, equilibrium arsenic solution was moved into sample vials and analyzed using an atomic fluorescence spectrometer (AFS 933, Beijing Titan instruments CO., Ltd, China) and inductively coupled plasma optical emission

spectrometer (ICP-OES, Optima 5300V, PerkinElmer, USA). Effects of pH, ionic strength, adsorbent dosage, and time were evaluated. All adsorption samples were shaken uniformly on the oscillator (HY-5, Changzhou Huanyu Scientific Instrument Factory, China) continuously. Solution samples were analyzed within 24 hours.

2.4. Adsorption Kinetic and Isothermal Tests

2.4.1. Adsorption Result Calculations. Arsenic removal rate and As adsorbed on manufactured materials can be calculated by the following equations:

$$\text{arsenic removal rate } (\%) = \frac{C_1 - C_2}{C_1} \times 100, \tag{1}$$

$$\text{adsorption capacity by a unit mass of adsorbent } (\text{As/adsorbent}\,(\text{mg/g})) = \frac{(C_1 - C_2)V}{M}, \tag{2}$$

where C_1 is the initial arsenic concentration (mg/L), C_2 is the arsenic concentration after adsorption (mg/L), V is the solution volume (L), and M is the adsorbent dosage (g).

2.4.2. Adsorption Kinetic Test. Two kinetic models were used to fit experimental data in order to explore adsorption rate which were the pseudo-first-order kinetic model and pseudo-second-order kinetic model.

The form of the pseudo-first-order kinetic model is [24]

$$\frac{dQ_t}{dt} = K_1 (Q_e - Q_t). \tag{3}$$

The following is its linear equation:

$$\ln (Q_e - Q_t) = \ln Q_e - \ln k_1. \tag{4}$$

The pseudo-second-order kinetic model can be expressed as [24]

$$\frac{dQ_t}{dt} = K_2 (Q_e - Q_t)^2. \tag{5}$$

Its linear equation is

$$\frac{t}{Q_t} = \frac{1}{K_2 Q_e^2} + \frac{t}{Q_e}, \tag{6}$$

where Q_e is adsorbed arsenic at adsorption equilibrium (mg/g), Q_t is adsorbed arsenic at any time (mg/g), K_1 and K_2 are the adsorption rate constants of pseudo-first-order kinetic (h^{-1}) and pseudo-second-order kinetic models, and t is the adsorption time (h). K_1 is calculated by fitting a straight line equation of $\ln (Q_e - Q_t) - t$, and the reaction rate increases in the rising of the k_1 value. K_2 is calculated by fitting a straight line equation of t/Q_t and t.

2.4.3. Adsorption Isothermal Test. Langmuir and Freundlich isotherm equations can be expressed as follows [25].

Langmuir equation:

$$\frac{C_e}{Q_e} = \frac{C_e}{Q_m} + \frac{1}{K_L Q_m}. \tag{7}$$

Freundlich equation:

$$lg (Q_e) = lg (K_F) + \frac{1}{n} lg (C_e), \tag{8}$$

where Q_e is adsorbed arsenic at adsorption equilibrium (mg/g), C_e is the arsenic concentration of adsorption equilibrium (mg/L), Q_m is the calculated constant related to adsorption capacity (mg/g), K_L is the Langmuir adsorption equilibrium constant related to the affinity of the binding sites and adsorption heat, K_F is the Freundlich constant, and n is the parameter that is related to adsorption strength. Larger K_F and n indicated that the adsorbent has better adsorption performance.

3. Results and Discussion

3.1. Material Characterization

3.1.1. XRD Diffraction Spectrum. The prepared adsorbent particles were exposed to complete XRD test. As is shown in Figure 1, the diffraction peaks of two adsorbents were 25.51°, 37.82°, 48.13°, 53.92°, and 75.13°, which showed a good consistency with the diffraction structure of TiO_2, according to the JCPDS standard card (no.71-1167); the crystal form of TiO_2 is anatase [26]. The peak which appeared at $2\theta = 26.6°$ was matched with the characteristic diffraction peak of SiO_2.

3.1.2. Transmission Electron Microscope and Scanning Electron Microscope Analysis. TEM image of the adsorbent is shown in Figure 2(a). The powdered activated carbon and nano-TiO_2 are interlaced. They showed an ellipsoid in shape and had uniform particle size. However, the partial region of the adsorbent displayed the aggregation of nanoparticles. From Figure 2(b), it was found that the part of supported nano-TiO_2 attached to the surface of activated carbon, and a small number of nano-TiO_2 entered into the channel of activated carbon. Supported TiO_2 exhibited a variety of particle sizes. Combined with the TEM image of the material, we concluded that supported nano-TiO_2 with the larger size was produced by agglomeration of small nano-TiO_2 particles. The average particle size of the adsorbent was around 52 nm.

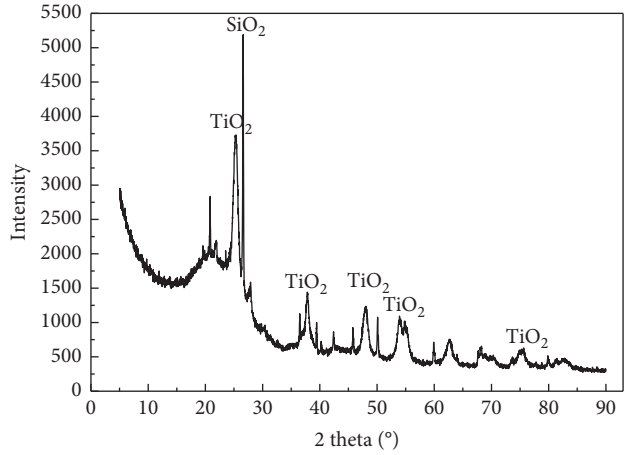

Figure 1: The XRD pattern of the adsorbent.

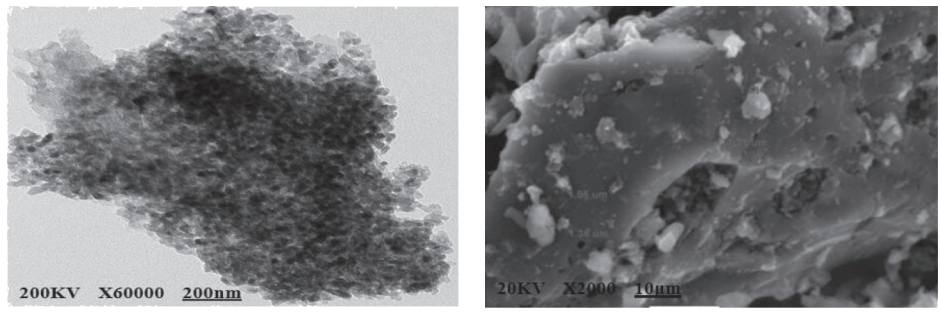

(a) (b)

Figure 2: (a) TEM and (b) SEM images of the adsorbent.

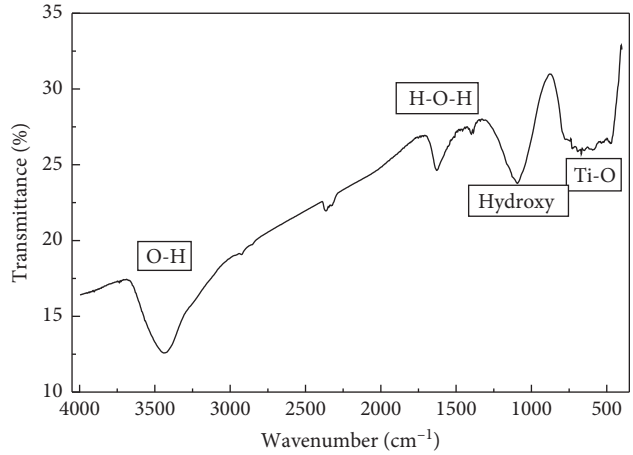

Figure 3: The infrared spectra of the adsorbent.

3.1.3. Fourier-Transform Infrared Spectra Analysis. The FTIR spectrum of the material is displayed in Figure 3. It showed the broad characteristic band at 3443.98 cm^{-1} which is assigned to O-H stretching vibration [19]. At around 1620 cm^{-1}, free water molecule H-O-H bending vibration was discovered [27]. Bending vibration of the hydroxyl group on the metal oxide occurs at 1060 cm−1 [28]. The broad wavenumber range around 500 cm^{-1} is attributed to the characteristic bonds of the Ti-O bond [29, 30].

3.1.4. BET Surface Area Analysis. The surface structure properties of the adsorbent were examined. The BET (Brunauer–Emmett–Teller) specific surface area was 371.17 m^2/g,

the pore volume of the adsorbent was 0.35 cm^3/g, and the pore size diameter was 11.70 nm.

3.1.5. TiO_2 Amount Loaded Test. After the precise determination and calculation of the load of TiO_2, the average load of TiO_2 was 179.50 mg/g (see Table S1).

3.2. Arsenic Removal in Batch Tests

3.2.1. The Effect of pH. The effect of pH on As(III) and As(V) removal was determined at pH ranging from 3 to 11. In Figure 4, it can be found that arsenic adsorption was strongly influenced by pH. Arsenic removal rate enhanced with increasing pH and then exhibited downward trends until pH = 11. pH is one of the important influencing factors in arsenic removal process [31]. Surface charge of the adsorbent and arsenic compound forms would be influenced by pH variation, thus affecting arsenic adsorption [32, 33].

There has been a slight rise in the removal rate of As(V) from 90.88% to 99.00% in a pH range 3 to 8. And then, there is an obvious decrease of the removal rate of As(V) from 99.00% to 82.39% with increasing pH from 8 to 11. Similar tendency was shown to remove As(III), and removal rate increased from 82.05% to 93.78% until pH = 8 and then was found to slip to 81.07%, respectively.

Figure 5 shows the zeta potentials of TiO_2 in the presence of 50 μg/L As(V) or As(III). The points of zero charge pH (pH_{PZC}) for TiO_2 were obtained around 8.0, which is higher than $pH_{PZC} = 6.8 \pm 0.2$ reported by Dutta et al. [34]. Dutta et al. showed that the surface of TiO_2 is positively charged when $pH < pH_{PZC}$, and it is negatively charged when $pH > pH_{PZC}$. The reaction is as follows:

$$\begin{aligned} Ti^{IV} - OH + H^+ &\longrightarrow Ti^{IV} - OH_2^+, \quad pH < pH_{PZC} \\ Ti^{IV} - OH + OH^- &\longrightarrow Ti^{IV} - O^- + H_2O, \quad pH > pH_{PZC} \end{aligned} \tag{9}$$

It is noted that $H_2AsO_4^-$ and $HAsO_4^{2-}$ are the main forms of As(V) at pH 3~11, while As(III) mainly exists in the form of H_3AsO_3 molecules in nonalkaline environments. When pH is relatively low, the adsorption of As by nano-TiO_2 loaded mainly depends on the interaction between the negative charge and the positive charge because the surface of nano-TiO_2 has a positive charge. Therefore, the adsorption capacity of As(V) is better than As(III). And in weak alkaline environment, H_3AsO_3 gradually transforms into anionic $H_2AsO_3^-$ by protonation effect, supported nano-TiO_2 will produce more adsorption sites with positive charge by removing the hydroxyl ion, and thus, more As(III) was adsorbed [34]. With the increase of pH, however, the adsorption capacity of As(V) and As(III) is gradually equal. At $pH > pH_{PZC}$, the surface of nano-TiO_2 is negatively charged. The advantages of surface charge adsorption gradually weakened, but there was still 80% As(V) and As(III) removal rate. Thus, it can be inferred that the surface complexation plays a certain role in the absorption of arsenic when pH is relatively high [35, 36]. Similar phenomenon has been observed for the adsorption of As(V) and As(III) onto nano-TiO_2-impregnated chitosan [37] and nano-TiO_2/feldspar-embedded chitosan beads [38].

When pH > 8, removal rate was decreased because the portion of positive charge of the adsorbent surface decreases, and the competitive adsorption of OH^- and arsenic compounds occurs, which was expected that arsenic desorption can be achieved in strong acidic or alkaline solution [39]. From pH 4 to 11, adsorption tendency of As(V) and As(III) was similar due to photocatalytic oxidation of TiO_2 in the presence of dissolved oxygen and light [40]. Based on our results, pH = 8 was the optimal adsorption condition for removing arsenic.

3.2.2. The Effect of the Adsorbent Dosage. The effect of the adsorbent dosage on the removal result is shown in Figure 6(a). It can be found that As(III) and As(V) removal efficiencies were strongly influenced by adsorbent dosage; 0.5 g dosage was sufficient to reach adsorption equilibrium when the initial arsenic concentration was 1.3 mg/L. The materials were significantly efficient in As(V) adsorption than As(III) in equivalent adsorbent level. The removal rate of arsenic was enhanced with increasing adsorbent dosage, but adsorption capacity decreased; a steep change occurred when adsorbent dosage increased from 0.01 to 0.50 g, and then a constant removal result was maintained with further increasing the adsorbent dosage in the adsorption process. When 0.5 g adsorbent was added into 25 mL arsenic solution, more than 93.00% As(III) and 95.00% As(V) were adsorbed, but amounts of arsenic adsorption of As(III) and As(V) were 0.0549 mg/g and 0.0649 mg/g, respectively. When dosage was less than 0.5 g, amounts of arsenic adsorbed experienced a sharp decrease and then reached equilibrium. It can be concluded that a high adsorbent dosage will lead to a high removal rate and a low adsorption capacity before adsorption equilibrium is reached, since the adsorption sites increased with rising adsorbent dosage which causes higher removal rate, but the total amount of arsenic adsorption remained unchanged significantly during the adsorption process. More adsorption sites were produced when the adsorbent dosage increased from 0.5 to 3 g, but these adsorption sites cannot be fully utilized. Genç et al. observed a similar phenomenon in removing arsenate by neutralized red mud [41]. Mohan and Gandhimathi [42] observed that heavy metal removal increased with an increasing adsorbent dose from 0.5 up to 2 g/L and remained almost constant thereafter and concluded that it was due to the saturation of the adsorbent sites by adsorbing the metal ions at the mass of the adsorbent which was 2 g/L, but they did not realize the opposite variation tendency of removal rate and adsorption capacity.

3.2.3. The Effect of Ionic Strength. In this section, the effect of ionic strength was investigated, and the result is shown in Figure 6(b). It was clear that As(III) adsorption was more dependent on ionic strength than As(V). In the adsorption process, arsenic removal efficiency had an increasing tendency as ionic strength increases to 0.5 mol/L. The removal

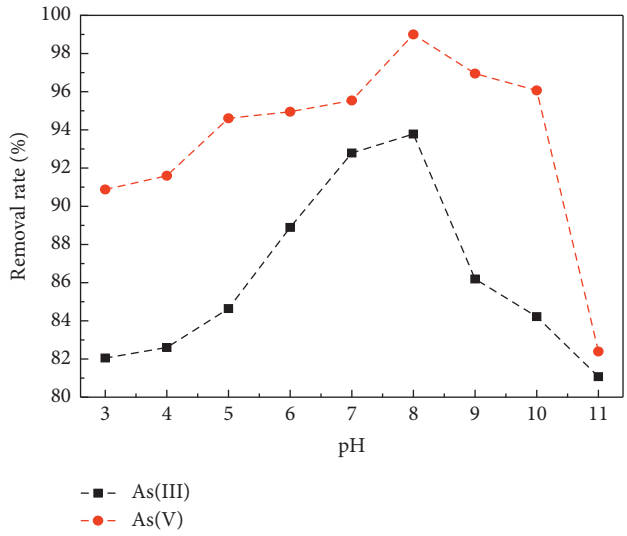

Figure 4: The effect of pH on arsenic removal at room temperature with reaction conditions: pH = 8, initial concentration: As(III) 70 μg/L and As(V) 84 μg/L, solution volume 25 ml, adsorbent dosage 0.05 g, and ionic strength 0.01 mol/L.

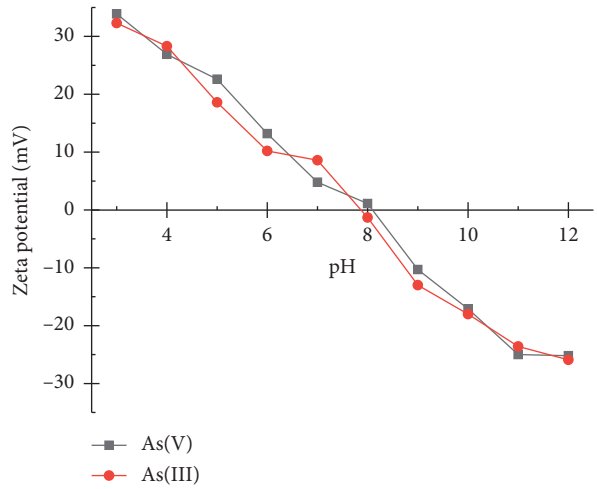

Figure 5: Zeta potential of nano-TiO_2 loaded as a function of pH with reaction conditions: initial concentration: As(III) 70 μg/L and As(V) 84 μg/L, solution volume 25 ml, adsorbent dosage 0.05 g, and ionic strength 0.01 mol/L.

rate of As(III) increased from 90.89% to 93.98%. The As(V) removal rate increased from 94.82% to 96.93%. The fact can be caused by hydroxyl groups of nano-TiO_2, and arsenic was linked by the ligand exchange reaction and formed inner surface complexes [43]. However, in the experiment for investigating the influence of ionic strength on arsenic adsorption, the opposite result was obtained from other researchers. (Anirudhan et al.) [19]. They noticed that As(V) adsorption percentage decreased as ionic strength increased and deemed the competition of chloride ions with As(V) which was the primary cause of the phenomenon.

3.2.4. Adsorption Kinetics. Adsorption kinetic experiments were conducted to determine the rate of arsenic removal. The experiment results are presented in Figure 7. It was showed that arsenic removal rate was enhanced with increasing adsorption time before adsorption equilibrium was reached. Compared to As(III), As(V) removal rate increased at a quick pace. The As(V) removal rate remains relatively constant within 70 minutes (1.17 hours) to 1440 minutes (24 hours) under the current experimental system. The adsorption of As(III) reached equilibrium at about 600 minutes (10 hours).

According to equation (4), graphs of In $(Q_e - Q_t)$ against t are presented in Figure 8. Adsorption kinetic parameters are shown in Table S2. The correlation coefficients of adsorbing As(V) and As(III) were 0.9683 and 0.9366, respectively. The correlation coefficient is in accord with the following order: As(V) > As(III). The pseudo-first-order kinetic model can describe the adsorption data of As(V) and As(III) at the current environment. Therefore, we concluded that physical adsorption could not be ignored in the arsenic removal process. Adsorption rate constant K_1

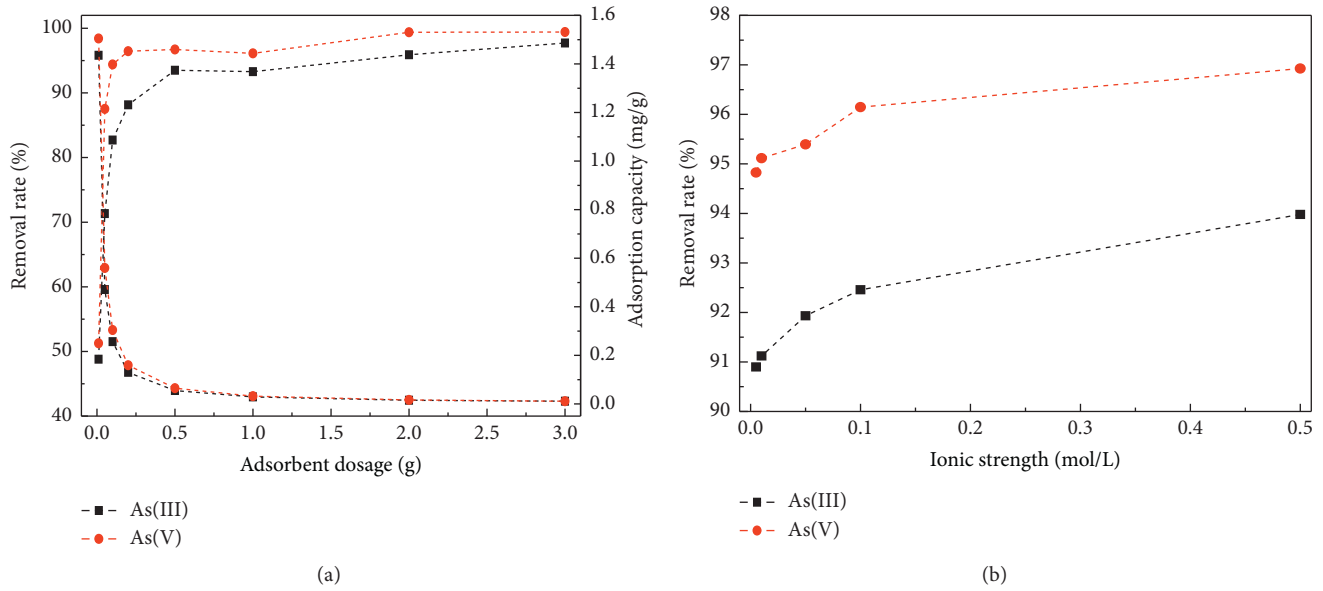

Figure 6: The effects of adsorbent dosage and ionic strength on arsenic removal at room temperature with reaction conditions: pH = 8, initial As concentration 1.3 mg/L, and solution volume 25 ml. (a) Adsorbent dosage (g). (b) Ionic strength (mol/g).

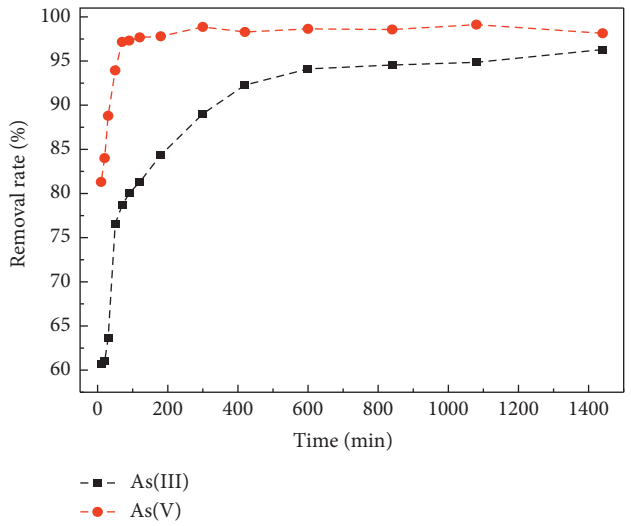

Figure 7: Adsorption kinetics of arsenic at room temperature with reaction conditions: pH = 8, initial As concentration 1.3 mg/L, ionic strength 0.5 mol/L, solution volume 25 ml, and adsorbent dosage 0.5 g.

follows order As(V) > As(III), which reveals that the adsorption rate of As(V) was faster than As(III). Experimental data were consistent with the information reflected by the K_1 value.

The pseudo-second-order kinetic plots are shown in Figure 9, and related parameters are presented in Table S2. Adsorption data can be well described by the pseudo-second-order model. The achieved correlation coefficients were higher than 0.9990. The correlation coefficients were present in the order As(V) > As(III). K_2 follows the order As(V) > As(III).

Compared to the pseudo-first-order model, it is obvious that the pseudo-second-order model fitted experimental data perfectly, which reveals that arsenic adsorption is a complex process because the pseudo-second-order model indicates the whole process of arsenic adsorption [44]. Excellent effect of adsorbing arsenic was reached by physical adsorption and chemical adsorption; chemical bonds are the main influencing factors in the chemical adsorption process [45].

3.2.5. Adsorption Isotherms. The adsorption isotherm experiments were carried at different initial concentrations ranging from 0.20 to 562.10 mg/L. The experiment results are presented in Figure 10. According to isotherm results,

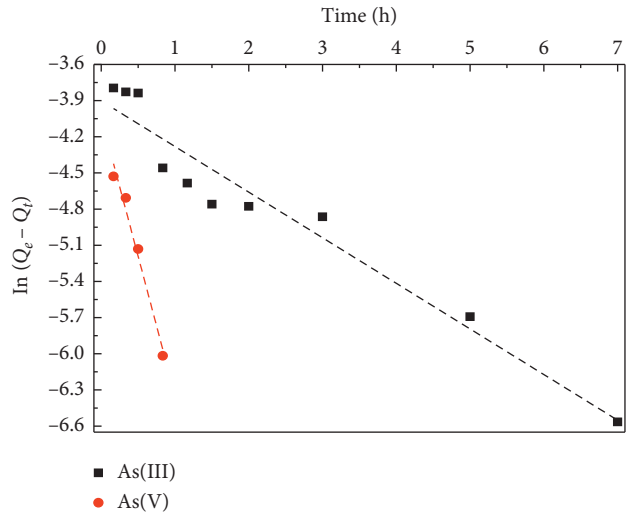

Figure 8: The pseudo-first-order kinetic plots for As(III) and As(V) removal at pH = 8, adsorbent dosage 0.5 g, and initial arsenic concentration 1.3 mg/L.

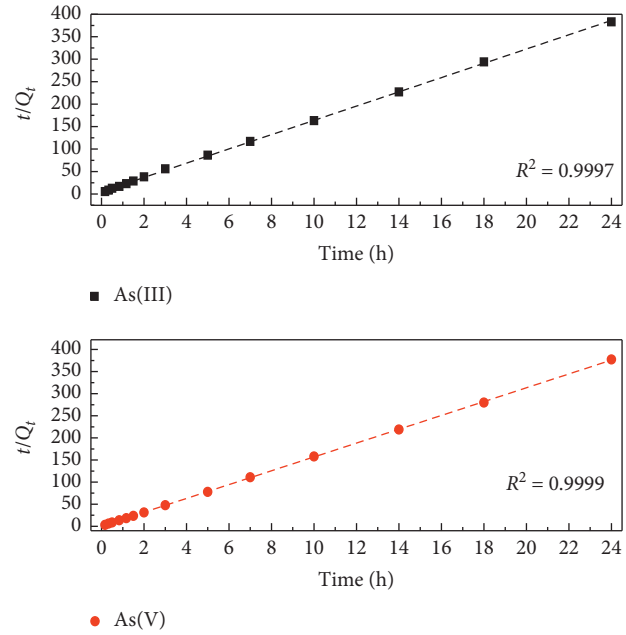

Figure 9: The pseudo-second-order kinetic plots for removal of As(III) and As(V) at pH = 8, adsorbent dosage 0.5 g, and initial arsenic concentration 1.3 mg/L.

the maximum adsorption capacities were 13.3800 mg/g and 15.1800 mg/g in As(III) and As(V), respectively. Compared to many adsorbents, the new materials had a more excellent adsorption capacity. Pena et al. [40] found that 8.30 mg/g As(III) and 11.20 mg/g As(V) were removed by nanocrystalline TiO_2. Altundoğan et al. [46] detected the maximum adsorption capacities of red mud for As(III) and As(V) at 0.33 mg/g and 0.35 mg/g, respectively.

The Freundlich and Langmuir parameters are given in Table S3. The isotherms are shown in Figures 11 and 12. The results indicated that arsenic adsorption data fitted the Freundlich isotherm preferably compared to the Langmuir isotherm, and the corresponding good correlation coefficient values were between 0.9600 and 0.9660, which indicated that arsenic adsorption by two adsorbents was heterogeneous adsorption on the nonuniform surface. The n values of the Freundlich equation were larger than 1, indicating that the adsorption of arsenic is favorable on the adsorbent. K_F of As (V) is larger than As(III) which reveals removal of As(V) is favorable than As(III). This conclusion is consistent with the results of John's research (2018).

3.3. Adsorption Mechanism. Arsenic removal from aqueous solution by the material adapted a process that physical

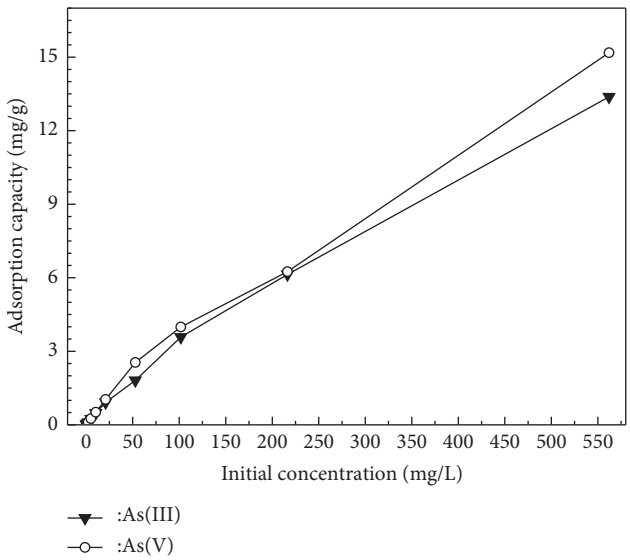

Figure 10: Adsorption isotherms of arsenic by TiO_2 at pH = 8, adsorbent dosage 0.5 g, and initial arsenic concentration 1.3 mg/L.

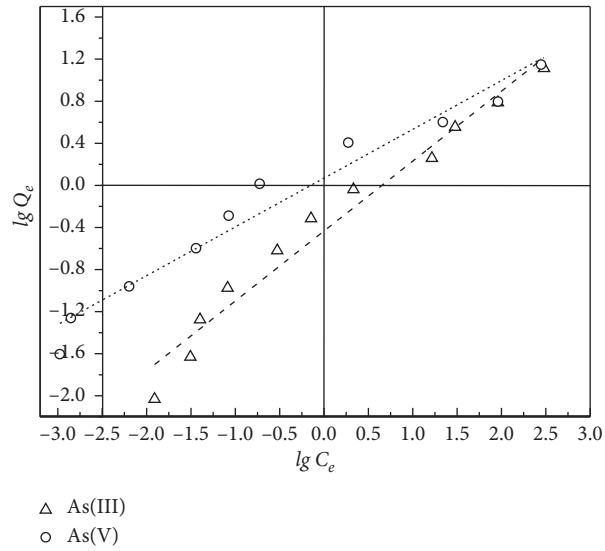

Figure 11: Freundlich model plots for the adsorption of As(III) and As(V) at pH = 8, adsorbent dosage 0.5 g, and initial arsenic concentration 1.3 mg/L.

adsorption and chemical adsorption coexist. From the perspective of the material itself, the adsorption of activated carbon on arsenic is mainly physical adsorption and is accompanied by chemical adsorption. Many researchers have found that the adsorption of nano-TiO_2 to As is an endothermic reaction and entropy-driven process [38, 47, 48]. According to the calculation of thermodynamic parameters, it can be inferred that the adsorption of nano-TiO_2 is mainly physical adsorption [49, 50]. However, the pseudo-second-order model fitted experimental data perfectly, and the isotherm model also fitted experimental data good which also indicated the important role of chemical forces in adsorption. Thus, it can be inferred that there are both physisorption and chemisorption in the process of carbon-supported nano-TiO_2 adsorption of arsenic. Sufficient adsorption sites provided a possibility for arsenic removal. As(V) mainly exists in the anion group when pH = 8 and was more adsorbed by activated carbon-supported nano-TiO_2 through electrostatic interaction because the surfaces of this material is positively charged at this time. Hydroxyl groups on the material surface were involved in arsenic sorption. The activated carbon-supported nano-TiO_2 can produce more absorption sites with positive charge by removing hydroxyl ion, and thus more As(III) was adsorbed [34]. At the same time, nano-TiO_2 loaded can finish the partial conversion of As(III) to As(V) because of the catalytic oxidation activity of TiO_2, and arsenic was adsorbed by forming monodentate or bidentate complexes at the surface of TiO_2 [51, 52]. In the adsorption process, As-O-AsO_4^{3-} and As -O-$H_2AsO_4^-$ groups formed in As(V) removal by nano-TiO_2 with the anatase crystal, and As-O-AsO_3^{3-} and As-O-$HAsO_4^{2-}$ were

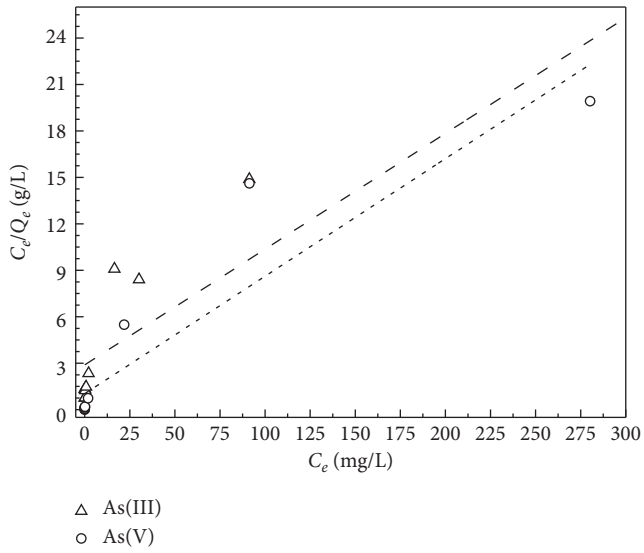

Figure 12: Langmuir model plots for the adsorption of As(III) and As(V) at pH = 8, adsorbent dosage 0.5 g, and initial arsenic concentration 1.3 mg/L.

found under light conditions in As(III) removal, both As(V) and As(III) were absorbed by forming the As-O-Ti and As-O bonds with TiO_2 [18]. In addition, arsenic removal by activated carbon was not neglected. Therefore, adsorption of arsenic on the adsorbent was mainly influenced by complexion formation.

4. Conclusions

The new adsorbent carbon substrate-supported nano-TiO_2 was synthesized using the sol-gel method, and its physical structure was further examined. This material had a high adsorption capacity for arsenic in weak alkaline solution, and the maximum adsorption capacity appeared at pH = 8. Increased amounts of arsenic were adsorbed by increasing ionic strength. Arsenic removal rate increased with increasing adsorbent dosage before the adsorption equilibrium was reached. The material exhibited a higher ability in removing As(V) than As(III). Adsorption kinetics and adsorption isotherm can be described well by the pseudo-second-order kinetic equation and Freundlich isotherm model, respectively. Arsenic adsorption equilibrium was achieved within 10 hours. The material can directly adsorb As(III), and it can also adsorb As(V), converted by photocatalysis.

Data Availability

The data used to support the findings of this study are available from the corresponding author upon request.

Additional Points

(i) The new arsenic-removing adsorbent material with high Ti loading was synthesized.

(ii) Excellent arsenic-removing capacity was observed. 15.1800°mg/g As(V) and 13.3800°mg/g As(III) were adsorbed by carbon substrate-supported nano-TiO_2.

Conflicts of Interest

The authors declare that there are no conflicts of interest regarding the work described in this paper.

Acknowledgments

The authors would like to express their sincere gratitude to Dr. Jiwei Hu (Guizhou Normal University) for providing language help. The authors greatly appreciate the financial support from the National Natural Science Foundation (21467005), Science and Technology Department from Guizhou Province (nos. LH(2014)7383 and (2016)1071), and Student's Platform for Innovation and Entrepreneurship Training Program (201510672003).

Supplementary Materials

Table S1: metal oxide amount loaded in the adsorbent. Table S2: the pseudo-first-order and the pseudo-second-order kinetic parameters for arsenic removal. Table S3: Freundlich and Langmuir isotherm constants. (*Supplementary Materials*)

References

[1] J. F. Ferguson and J. Gavis, "A review of the arsenic cycle in natural waters," *Water Research*, vol. 6, no. 11, pp. 1259–1274, 1972.

[2] Y. Wu, X.-Y Zhou, M. Lei et al., "Migration and transformation of arsenic: contamination control and remediation in realgar mining areas," *Applied Geochemistry*, vol. 77, pp. 44–51, 2017.

[3] M. Yu, "Colorimetric detection of trace arsenic(III) in aqueous solution using arsenic aptamer and gold nanoparticles," *Australian Journal of Chemistry*, vol. 67, no. 5, p. 813, 2014.

[4] T. Luo and J. Yu, "S17 the effect of phosphate and sulfate on arsenate desorption from nano-TiO 2," *Journal of Residuals Science & Technology*, vol. 12, pp. S17–S23, 2015.

[5] M. Tuzen, K. O. Saygi, I. Karaman, and M. Soylak, "Selective speciation and determination of inorganic arsenic in water, food and biological samples," *Food and Chemical Toxicology*, vol. 48, no. 1, p. 41, 2010.

[6] P. L. Smedley and D. G. Kinniburgh, "A review of the source, behaviour and distribution of arsenic in natural waters," *Applied Geochemistry*, vol. 17, no. 5, pp. 517–568, 2002.

[7] M. Berg, H. C. Tran, T. C. Nguyen et al., "Arsenic contamination of groundwater and drinking water in vietnam: a human health threat," *Environmental Science & Technology*, vol. 35, no. 13, pp. 2621–2626, 2001.

[8] B. A. Manning and S. Goldberg, "Adsorption and stability of arsenic(III) at the clay Mineral–Water interface," *Environmental Science & Technology*, vol. 31, no. 7, pp. 2005–2011, 1997.

[9] M. L. Li and C. B. Moore, "Adsorption of arsenite on amorphous iron hydroxide from dilute aqueous solution,"

Environmental Science & Technology, vol. 14, no. 2, pp. 214–216, 1980.

[10] G. Yu, D. Sun, and Y. Zheng, "Health effects of exposure to natural arsenic in groundwater and coal in China: an overview of occurrence," *Environmental Health Perspectives*, vol. 115, no. 4, pp. 636–642, 2007.

[11] G. Chen, "Electrochemical technologies in wastewater treatment," *Separation and Purification Technology*, vol. 38, no. 1, pp. 11–41, 2004.

[12] A. Dabrowski, Z. Hubicki, P. Podkościelny, and E. Robens, "Selective removal of the heavy metal ions from waters and industrial wastewaters by ion-exchange method," *Chemosphere*, vol. 56, no. 2, pp. 91–106, 2004.

[13] F. Fu and Q. Wang, "Removal of heavy metal ions from wastewaters: a review," *Journal of Environmental Management*, vol. 92, no. 3, pp. 407–418, 2011.

[14] T. A. Kurniawan, G. Y. S. Chan, W.-H. Lo, and S. Babel, "Physico-chemical treatment techniques for wastewater laden with heavy metals," *Chemical Engineering Journal*, vol. 118, no. 1-2, pp. 83–98, 2006.

[15] D. Mohan and P. C. Pittman, "Arsenic removal from water/wastewater using adsorbents--A critical review," *Journal of Hazardous Materials*, vol. 142, no. 1-2, pp. 1–53, 2007.

[16] G. Yan and T. Viraraghavan, "Heavy-metal removal from aqueous solution by fungus Mucor rouxii," *Water Research*, vol. 37, no. 18, pp. 4486–4496, 2003.

[17] A. Demirbas, "Heavy metal adsorption onto agro-based waste materials: a review," *Journal of Hazardous Materials*, vol. 157, no. 2-3, pp. 220–229, 2008.

[18] L. Ma and S. X. Tu, "Removal of arsenic from aqueous solution by two types of nano TiO2 crystals," *Environmental Chemistry Letters*, vol. 9, no. 4, pp. 465–472, 2011.

[19] T. S. Anirudhan, L. Divya, and J. Parvathy, "Arsenic adsorption from contaminated water on Fe(III)-coordinated amino-functionalized poly (glycidylmethacrylate)-grafted TiO_2-densified cellulose," *Journal of Chemical Technology & Biotechnology*, vol. 88, no. 5, pp. 878–886, 2013.

[20] H. Cao, B. Li, J. Zhang, F. Lian, X. Kong, and M. Qu, "Synthesis and superior anode performance of TiO2@reduced graphene oxide nanocomposites for lithium ion batteries," *Journal of Materials Chemistry*, vol. 22, no. 19, pp. 9759–9766, 2012.

[21] S. Bang, M. Patel, L. Lippincott, and X. Meng, "Removal of arsenic from groundwater by granular titanium dioxide adsorbent," *Chemosphere*, vol. 60, no. 3, pp. 389–397, 2005.

[22] X. Long and S. Tu, "Removal of arsenic from water by nano titanium dioxide doped with activated carbon," *Industrial Water Treatment*, vol. 32, no. 4, pp. 29–32, 2012.

[23] L. I. Rong, X. Xiao, and C. Wang, "Photocatalytic degradation of gaseous acetone using TiO_2 nanoparticles supported on activated carbon," *Materials Review*, vol. 25, pp. 68–71, 2011.

[24] P. Pillewan, S. Mukherjee, T. Roychowdhury, S. Das, A. Bansiwal, and S. Rayalu, "Removal of As(III) and As(V) from water by copper oxide incorporated mesoporous alumina," *Journal of Hazardous Materials*, vol. 186, no. 1, p. 367, 2011.

[25] X. Fan, D. J. Parker, and M. D. Smith, "Adsorption kinetics of fluoride on low cost materials," *Water Research*, vol. 37, no. 20, p. 4929, 2003.

[26] I. R. Bellobono, A. Carrara, B. Barni, and A. Gazzotti, "Laboratory- and pilot-plant-scale photodegradation of chloroaliphatics in aqueous solution by photocatalytic membranes immobilizing titanium dioxide," *Journal of Photochemistry and Photobiology A: Chemistry*, vol. 84, no. 1, pp. 83–90, 1994.

[27] Y. Guo, Z. Zhu, Y. Qiu, and J. Zhao, "Synthesis of mesoporous Cu/Mg/Fe layered double hydroxide and its adsorption performance for arsenate in aqueous solutions," *Journal of Environmental Sciences*, vol. 25, no. 5, pp. 944–953, 2013.

[28] Z. Li, S. Deng, G. Yu, J. Huang, and V. C. Lim, "As(V) and As(III) removal from water by a Ce-Ti oxide adsorbent: behavior and mechanism," *Chemical Engineering Journal*, vol. 161, no. 1-2, pp. 106–113, 2010.

[29] S. Abbasizadeh, A. R. Keshtkar, and M. A. Mousavian, "Sorption of heavy metal ions from aqueous solution by a novel cast PVA/TiO_2 nanohybrid adsorbent functionalized with amine groups," *Journal of Industrial and Engineering Chemistry*, vol. 20, no. 4, pp. 1656–1664, 2014.

[30] J.-P. Nikkanen, T. Kanerva, and T. Mäntylä, "The effect of acidity in low-temperature synthesis of titanium dioxide," *Journal of Crystal Growth*, vol. 304, no. 1, pp. 179–183, 2007.

[31] S. Bekkouche, S. Baup, M. Bouhelassa, S. MolinaBoisseau, and C. Petrier, "Competitive adsorption of phenol and heavy metal ions onto titanium dioxide (Dugussa P25)," *Desalination & Water Treatment*, vol. 37, no. 1-3, pp. 364–372, 2012.

[32] H. Park and W. Choi, "Effects of TiO_2 Surface fluorination on photocatalytic reactions and photoelectrochemical behaviors," *The Journal of Physical Chemistry B*, vol. 108, no. 13, pp. 4086–4093, 2004.

[33] B. Peng, T. Song, T. Wang et al., "Facile synthesis of Fe 3 O 4 @Cu(OH) 2 composites and their arsenic adsorption application," *Chemical Engineering Journal*, vol. 299, pp. 15–22, 2016.

[34] P. K. Dutta, A. K. Ray, V. K. Sharma, and F. J. Millero, "Adsorption of arsenate and arsenite on titanium dioxide suspensions," *Journal of Colloid and Interface Science*, vol. 278, no. 2, pp. 270–275, 2004.

[35] Y. John, V. E. David, and D. Mmereki, "A comparative study on removal of hazardous anions from water by adsorption: a review," *International Journal of Chemical Engineering*, vol. 2018, pp. 1–21, 2018.

[36] S. Kong, Y. Wang, H. Zhan, S. Yuan, M. Yu, and M. Liu, "Adsorption/oxidation of arsenic in groundwater by nanoscale Fe-Mn binary oxides loaded on zeolite," *Water Environ. Res.* vol. 86, no. 2, pp. 147–155, 2014.

[37] S. M. Miller and J. B. Zimmerman, "Novel, bio-based, photoactive arsenic sorbent: TiO_2-impregnated chitosan bead," *Water Research*, vol. 44, no. 19, pp. 5722–5729, 2010.

[38] M. Yazdani, A. Bhatnagar, and R. Vahala, "Synthesis, characterization and exploitation of nano-TiO_2/feldspar-embedded chitosan beads towards UV-assisted adsorptive abatement of aqueous arsenic (As)," *Chemical Engineering Journal*, vol. 316, pp. 370–382, 2017.

[39] T.-F. Lin and J.-K. Wu, "Adsorption of arsenite and arsenate within activated alumina grains: equilibrium and kinetics," *Water Research*, vol. 35, no. 8, pp. 2049–2057, 2001.

[40] M. E. Pena, G. P. Korfiatis, M. Patel, L. Lippincott, and X. Meng, "Adsorption of As(V) and As(III) by nanocrystalline titanium dioxide," *Water Research*, vol. 39, no. 11, pp. 2327–2337, 2005.

[41] H. Genç, J. C. Tjell, D. Mcconchie, and O. Schuiling, "Adsorption of arsenate from water using neutralized red mud," *Journal of Colloid and Interface Science*, vol. 264, no. 2, pp. 327–334, 2003.

[42] S. Mohan and R. Gandhimathi, "Removal of heavy metal ions from municipal solid waste leachate using coal fly ash as an adsorbent," *Journal of Hazardous Materials*, vol. 169, no. 1-3, pp. 351–359, 2009.

[43] Z. J. Chen, H. N. Liu, and H. F. Zhang, "Research progress on mechanisms about the effect of ionic strength on adsorption," *Environmental Chemistry*, vol. 29, no. 6, pp. 997–1003, 2010.

[44] U. Farooq, J. A. Kozinski, M. A. Khan, and M. Athar, "Biosorption of heavy metal ions using wheat based biosorbents-a review of the recent literature," *Bioresource Technology*, vol. 101, no. 14, pp. 5043–5053, 2010.

[45] Y.-S. Ho, "Second-order kinetic model for the sorption of cadmium onto tree fern: a comparison of linear and non-linear methods," *Water Research*, vol. 40, no. 1, pp. 119–125, 2006.

[46] H. S. Altundoğan, S. Altundoğan, F. Tümen, and M. Bildik, "Arsenic removal from aqueous solutions by adsorption on red mud," *Waste Management*, vol. 20, no. 8, pp. 761–767, 2000.

[47] M. R. Mafra, L. Igarashi-Mafra, D. R. Zuim, É im. Vasques, and M. A. Ferreira, "Adsorption of Remazol brilliant blue on an orange peel adsorbent," *Brazilian Journal of Chemical Engineering*, vol. 30, no. 3, pp. 657–665, 2013.

[48] R. C. I. Fontan, L. A. Minim, R. C. F. Bonomo, L. H. M. da Silva, and V. P. R. Minim, "Adsorption isotherms and thermodynamics of α-lactalbumin on an anionic exchanger," *Fluid Phase Equilibria*, vol. 348, pp. 39–44, 2013.

[49] Z. Bekçi, Y. Seki, and M. Kadir Yurdakoç, "A study of equilibrium and FTIR, SEM/EDS analysis of trimethoprim adsorption onto K10," *Journal of Molecular Structure*, vol. 827, no. 1-3, pp. 67–74, 2007.

[50] D. Zhang, H. Niu, X. Zhang, Z. Meng, and Y. Cai, "Strong adsorption of chlorotetracycline on magnetite nanoparticles," *Journal of Hazardous Materials*, vol. 192, no. 3, pp. 1088–1093, 2011.

[51] G. He, M. Zhang, and G. Pan, "Influence of pH on initial concentration effect of arsenate adsorption on TiO_2 surfaces: thermodynamic, DFT, and EXAFS interpretations," *The Journal of Physical Chemistry C*, vol. 113, no. 52, pp. 21679–21686, 2009.

[52] M. Pena, X. Meng, G. P. Korfiatis, and C. Jing, "Adsorption mechanism of arsenic on nanocrystalline titanium dioxide," *Environmental Science & Technology*, vol. 40, no. 4, pp. 1257–1262, 2006.